The effect of effusion holes inclination angle on the adiabatic film cooling effectiveness in a three-sector gas turbine combustor rig with

https://doi.org/10.1016/j.ijthermalsci.2017.07.003

The Effect of Effusion Holes Inclination Angle on the Adiabatic Film Cooling Effectiveness in a Three-Sector Gas Turbine Combustor Rig with a Realistic Swirling Flow

Antonio Andreini[a,*], Riccardo Becchi[a], Bruno Facchini[a], Alessio Picchi[a], Antonio Peschiulli[b]

[a] *Department of Industrial Engineering DIEF, University of Florence, Via di Santa Marta 3, 50139 Florence, Italy*
[b] *GE Avio S.R.L. - Via I Maggio, 99, 10040, Rivalta di Torino (TO), Italy*

Abstract

The introduction of Lean Burn concept as basic Low-NO_x scheme for future aero-engines is heavily affecting the aero-thermal design of combustors. A great amount of air is admitted through the injection system with relevant swirl components, producing very complex flow structures (recirculations, vortex breakdown) for flame stabilization. As a consequence a reduced quantity of air is available for liner cooling, pushing the adoption of high effectiveness cooling schemes. Effusion cooling represents one of the first choices due to its low weight and a relatively easy manufacturability. Liner metal temperature is kept low by the combined protective effect of coolant film, heat removal inside holes and an improved cold-side convection. In lean burn systems the evolution of film protection can be heavily influenced by the swirl flow interaction with combustor walls.

The subject of this work is to investigate the effects of the realistic flow field of a lean burn injector on the adiabatic film cooling effectiveness on an effusion cooled combustor liner. A dedicated three-sector rig was designed with the aim of measuring film effectiveness with Pressure Sensitive Paint technique. Three effusion cooling geometries with different inclination angles were tested at various levels of pressure drops across the perforation, resulting in different blowing ratio values. It was also taken into consideration several flow rate levels of starter film realized by spent dome cooling air, injected through a dedicated plain slot. The analysis of film effectiveness measurements were supported by flow field investigation in the near wall region carried out by means of Particle Image Velocimetry.

Results pointed out the relevant impact of combustor flow field on the adiabatic film cooling effectiveness as well as a significant role of the inclination angle, recommending a careful revision of standard design practices based on one dimensional flow assumption and suggesting possible holes arrangement optimization.

Keywords: Gas Turbine, Combustor, Liner, Effusion cooling, Adiabatic Film Cooling Effectiveness, Swirl flows, PSP, PIV

*Corresponding Author
Email address: antonio.andreini@unifi.it (Antonio Andreini)

Nomenclature

Acronyms

BR Blowing Ratio $[-]$

CCD Charged Coupled Device

Cd Discharge coefficient $[-]$

CR Corner Recirculation

DR Density Ratio $[-]$

IR Inner Recirculation

NO_x Nitrogen Oxides

$PERM$ Partial Evaporation and Rapid Mixing

PIV Particle Image Velocimetry

$PMMA$ Poly-Methyl Methacrylate

PSP Pressure Sensitive Paint

Re Reynolds number $[-]$

S_N Swirl Number $[-]$

Greek symbols

α Injection angle $[deg]$

η Film Cooling Effectiveness

σ Perforation porosity $[-]$

θ Tangential direction in swirler flow $[-]$

Latin symbols

$\dot{m}$ Mass flow $[g/s]$

A Area $[m^2]$

C Mass fraction $[-]$

D Diameter $[m]$

d Holes diameter $[m]$

G Momentum flux $[kg/m/s^2]$

P Static pressure $[Pa]$

S Hole pitch $[m]$

T Temperature $[K]$

V Velocity $[m/s]$

W Slot coolant consumption $[-]$

x Stream-wise, axial direction $[m]$

y Span-wise, lateral direction $[m]$

z Orthogonal to test plate direction $[m]$

Subscripts

ad adiabatic

aw adiabatic wall

$cool$ cooling flow

eff effusion flow

h hydraulic

in inlet

$main$ mainstream

max maximum

out outlet

$slot$ slot cooling system

sw swirler

w wall

x axial direction

y lateral direction

z orthogonal to test plate direction

1. Introduction

In modern gas turbine combustors the process of flame stabilization and anchoring is widely based on the use of swirling flows. Combustion air is delivered as swirling jets in single or multiple configurations. The objective is to promote the so-called vortex breakdown process, which is the base flow structure of swirl stabilized flames. With this type of flow, wide low speed regions are produced by the onset of inner and outer recirculations, supporting local flame anchoring. Recirculating flows allow to have a continuous supply of high temperature gases to incoming fresh mixture, while the strong velocity gradients and flow unsteadiness greatly enhance free stream turbulence which improves the overall reaction and mixing rates. This type of flame stabilization process has become more and more common and exasperated with the widespread use of lean flames for reduction of NO_x emissions, firstly adopted in heavy duty gas turbines [1], and more recently considered also for aero-engine combustors to fulfil the future emissions standards [2].

A common characteristics of lean burn gas turbine combustors is the great amount of air delivered by the fuel-air injection system, that can reach $70 - 75\%$ of total combustor air. This means a strong reduction of air available for liner wall cooling, forcing to the introduction of high effectiveness cooling schemes. Among different possible solutions, effusion cooling (or full coverage film cooling) certainly represents one of the most promising technology. It is based on the injection of cooling air through a dense pattern of small diameter holes drilled on the liner. The purpose is to generate an high effectiveness layer of coolant on the liner surface, avoiding its direct exposure to hot gases, and to provide heat removal by forced convection inside each hole. An additional positive contribution to overall cooling effectiveness may come to an increased convective heat transfer on the cold-side of the liner due to the suction effect of coolant flow near the rim of each effusion holes. Thanks to the relative simple manufacturing process involved and a reduced impact on combustor weight, effusion is one the first options, especially in aero-engine applications. A recent review on effusion cooling concept with a discussion about the basics related to hole spacing and coolant-hot-gas interaction can be found in Krewinkel [3], where some perspectives about the application of effusion cooling to turbine blade cooling are also reported. More specific assessments regarding the application of effusion cooling to combustor liner with fundamental analysis about the relative weight of the three main contributions to overall cooling effectiveness can be found in Martiny et al. [4] and more recently in Gerendás et al. [5] and Andreini et al. [6].

The engineering problem of applying effusion to combustor liner cooling, together with all related physical aspects, has been widely analysed over the last 40 years, with several contributions available in the open literature. In particular most part of the studies have usually been aimed at investigating the role of the various flow and geometric parameters on the film cooling effectiveness, generally with simplified configurations (flat plates with uniform mainstream flow). One of the first contribution is due to Kasagi et al. [7] where the overall cooling effectiveness of full coverage film cooling plates was measured at different blowing ratios with liquid crystals technique. The focus was put on the the role of thermal properties of the plate material. Among the pioneering studies it is worth to cite the contributions by Andrews and co-workers [8, 9, 10] where the effects on film effectiveness of several parameters, as the number of holes, length and arrangement, were investigated. In their study, Martiny et al. [11] evaluated row by row adiabatic film effectiveness (via Infra-Red thermography) and performed flow visualizations (by means of Schlieren photography) on a full coverage film cooling plate with highly inclined holes (17°) at different blowing ratios (0.5 to 4.0). It was observed that, even with high blowing ratio and therefore with full penetration of jets, an appreciable cooling benefit can be measured in terms of adiabatic film effectiveness. This is due to a reduction of gas temperature in the mixing region contributing to keep near wall temperature low even without the presence of a coherent film: this is expected to be the process in actual combustor where high blowing ratios are commonly observed.

An extensive parametric study was later realized by Gustafsson and Johansson [12] where overall cooling effectiveness was tested with Infra-Red thermography. A large database was obtained varying several flow and geometric parameters, nevertheless results in terms of overall cooling effectiveness do not permit to accurately separate the effects on adiabatic film effectiveness and heat transfer. In the contribution by Harrington et al. [13] the effect of an increasing free stream turbulence on the adiabatic film effectiveness was analysed for normal injection holes. A reduction of film coverage is observed when turbulence increases, but the impact is largely reduced with blowing ratios approaching 1.0. More recently Martin and Thorpe [14] observed an increase of adiabatic effectiveness with realistic high free stream turbulence when using inclined holes at blowing ratio above 1.0: this is due to an increased mixing rate of the jet with the mainstream, which enhance the amount of coolant close to wall region. The investigation carried out by Scrittore et al. [15] was focused on the measurement of adiabatic film effectiveness and flow field from inclined effusion cooling jets in a range of blowing ratios (3.2 to 5.0) that can be observed in actual combustors. A large number of effusion rows was considered (20) permitting to observe the achievement of fully developed film after the 15th row. In their recent study, Ligrani et al. [16] showed adiabatic film effectiveness and heat transfer for full coverage film cooling configurations in the presence of a streamwise pressure gradient; the effect of the blowing ratio and the influence of dense/sparse hole arrays on the thermal effectiveness are discussed.

One of the most important parameter affecting the final adiabatic film effectiveness of multi row effusion cooling is certainly the inclination angle of the holes. Among the first systematic studies concerning this aspect is worth to be mentioned Foster and Lampard [17] who analysed the effects of the injection angle investigating a set of geometries with $\alpha = 35°$, $55°$, $90°$. Great dependence from this parameter was observed, with small injection angle that showed the highest cooling effectiveness at low blowing ratios, while large injection angles were advantageous at high blowing ratios. Coming to more recent contributions, Hale et al. [18] performed a parametric study for a single row of short holes, fed by a narrow plenum, with two different injection angles (35° and 90°). Results highlighted that under specific conditions, similar or improved coverage was achieved with orthogonal injection compared with 35° holes. An investigation carried out by Baldauf et al. [19] indicated optimum flow conditions for efficient cooling for a wide range of configurations, among which it's worth to mention three different streamwise angle levels (30°, 60°, 90°). The same range of angles were investigated by Yuen and Martinez-Botas [20] in a flat plate test facility with a zero pressure gradient for a wide range of blowing ratios. Behrendt et al. [21] presented results about the characterization of the film effectiveness of advanced combustor cooling concepts at realistic operating conditions. They observed an effectiveness improvement at lower cooling hole angles (20°) due to the reduced penetration depth of the cooling air jets. More recently Andreini et al. [22] carried out an investigation on several multi-perforated plates measuring the adiabatic film effectiveness by using Pressure Sensitive Paint technique on a flat plate test rig. A comparison between 30° and 90° at different blowing ratios was discussed, pointing out the role of different free-stream turbulence levels and coolant to mainstream density ratio.

All the above mentioned works regarding effusion cooling are based on simple mainstream flow fields (i.e., uniform velocity). First attempts to take into account actual combustor flow field features are due for instance to Scrittore et al. [23] and later to Ceccherini et al. [24], where the interactions of effusion cooling flow with dilution jets or starter film cooling were investigated on single flat plate configurations. The use of high swirling flows for flame stabilization purposes may result in a great interaction between swirl jet and combustor liner, which can deeply affect both convective heat transfer and film cooling protection. Very few studies can be found in the open literature where the investigation of such effects are reported. It's worth to be recalled the pioneering studies realized at the Karlsruhe Institute of Techonology (KIT) [25, 26], where effusion cooling effectiveness in a three sector rig with realistic lean direct injection nozzles was measured by Infra-Red thermography. More recently, Andreini and co-workers [27, 28] carried out an experimental survey aimed at measuring adiabatic film cooling effectiveness and heat transfer coefficient in a planar three sector rig operated with a representative swirling flow field: a cooling scheme based on effusion with slot cooling was considered. In both studies, a specific configuration of multi-perforated liner was used, without a systematic deepening about the role of geometric parameters on cooling effectiveness. A similar investigation was recently carried out by Ge et al. [29] with Infra-Red thermography in reactive conditions but with a reduced number of effusion rows: the authors point out a complex measurement process in presence of the heat release due to combustion which affects the accuracy of the obtained results.

The aim of the present study is to deepen the knowledge on film cooling interaction with highly swirling flows in realistic combustor flow field environment, exploring the impact on adiabatic film cooling effectiveness when varying one of the most critical parameter: the coolant injection angle.

2. Experimental setup

2.1. Experimental geometry

Experiments were carried out in an open loop wind tunnel device reported installed at the THT-Lab of the University of Florence, Italy: schematic representation is reported in Figure 1. The test rig was developed within the European Research project LEMCOTEC (Low Emissions Core-Engine Technologies) [30] and consists of a planar three-sector combustor operating at ambient conditions without reactive processes. It is equipped with a complete cooling scheme composed of a slot system and multi-perforated liners whose

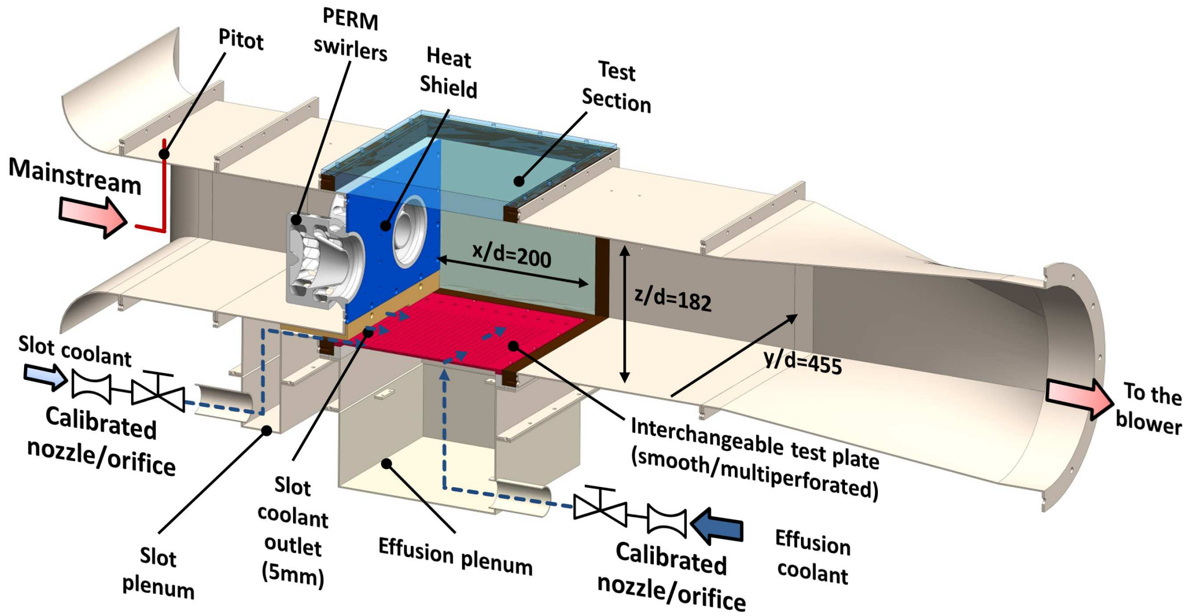

Figure 1: Cross sectional view of the test rig

mass flow rates can be controlled independently. The mainstream flow is delivered by three injectors which produce a flow field representative of a swirl stabilized combustor. Details of the swirler geometry will be discussed in a following section.

The experimental tests were designed to work at ambient pressure and near ambient temperature conditions, so allowing the use of Pressure Sensitive Paint (organic compound). An enlarged scale factor was selected with respect to reference engine in order to replicate Reynolds number and pressure drop of the swirlers with respect to the engine nominal conditions.

The mainstream flow is fed inside the test rig by means of a 90 kW centrifugal blower and enters inside the test section, which reproduces an aero-engine lean combustor, after being swirled by the injectors. The inner liner of the chamber is represented by a multi-perforated plate and is fed by an upstream large plenum

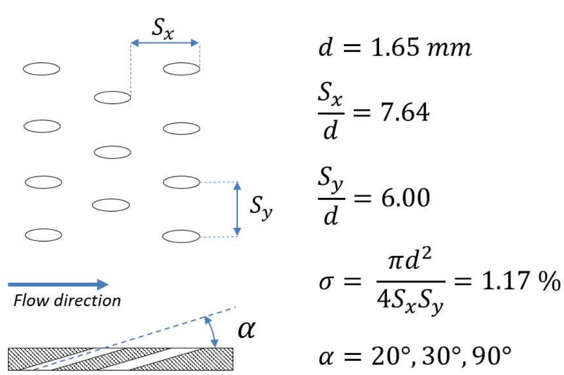

Figure 2: Summary of effusion perforation geometry

chamber. During the experimental campaign three different effusion liner geometries were investigated varying the holes injection angle (evaluated with respect to liner surface along nominal mainstream direction): tested angles are 20°, 30° and 90°. All the effusion plates share the same holes pattern: 1184 cylindrical holes are arranged in a staggered array counting for a total of 23 rows, with the first row located about $0.22S_x$ from the beginning of the liner. Scaled holes diameter is equal to $d = 1.65\ mm$ in all cases, while normalized streamwise and spanwise pitches are respectively $S_x/d = 7.64$ and $S_y/d = 6$. This common diameter and holes arrangement leads to a common plate porosity of about 1.17%: porosity is here defined as the ratio between holes aperture and overall plate surface. A summary of the principal geometric data of multiperforations is shown in Figure 2.
The slot exit is positioned on the dome wall below the three injectors. It has a constant height of $5mm$ and a width equal to 2 times the swirlers pitch. For both the cooling systems, air passes through screens and flow straighteners upstream of the injection, and the mass flow rates are set by adjusting two manual ball valves.

The test section has a length in the flow direction equal to $x/d = 200$, a width of $y/d = 455$ and an height of $z/d = 182$. The lateral walls and the top side of the chamber, located in opposite position with respect to the multi-perforated liner, are made in a transparent material (in this case Poly-Methyl MethAcrylate (PMMA)) in order to allow wide optical accesses for both adiabatic film cooling effectiveness tests and PIV measurements. Downstream of the test section, the mainstream and the mixed cooling flows pass through a constant cross-section channel and a smooth converging duct before flowing towards the silencer installed at the blower inlet.

The pressure drop across the swirlers and consequently the mainstream mass flow rate is imposed acting on the rotating speed of the centrifugal blower by means of an inverter. The mass flow rate is measured by means of a Pitot tube, located downstream of the rig inlet bell mouth, and double checked evaluating the injectors pressure drop, assumed as known the effective passage area. The uncertainty of the main mass flow measurement is ±6% with a level of confidence of 95%. Calibrated nozzles, installed in two dedicated feeding ducts positioned upstream of the coolant plena, are used to evaluate the slot and effusion mass flow rates with an uncertainty of ±5%. T type thermocouples (uncertainty $\pm 0.5\ K$ with level of confidence of 95%) are employed to monitor the flow temperature in several locations of the rig with the data acquisition provided by an HP/Agilent® 34972A unit. A pressure scanner Scanivalve®DSA 3217 with temperature compensated piezoresistive relative pressure sensors measures the static pressure in 13 different locations with a maximum uncertainty of $\pm 7\ Pa$ (level of confidence of approximately 95%).

2.2. Swirler geometry

The apparatus is characterized by the presence of three air spray swirlers designed by GE-Avio. The objective of the design is to realize a device capable of Ultra Low NO_x operations through a lean, swirl stabilized, spray flame [31]. The injectors, called PERM (Partial Evaporation and Rapid Mixing), are characterized by two radial co-rotating swirlers which have the role of producing a highly swirling flow at the outlet section of the nozzle (Figure 3). The final outcome is the achievement of a large inner recirculation region surrounded by an high velocity annular jet, which represents the main flow structures of typical swirl stabilized flames.

According to the review of Lilley [32], the onset of the vortex breakdown process, and the related presence

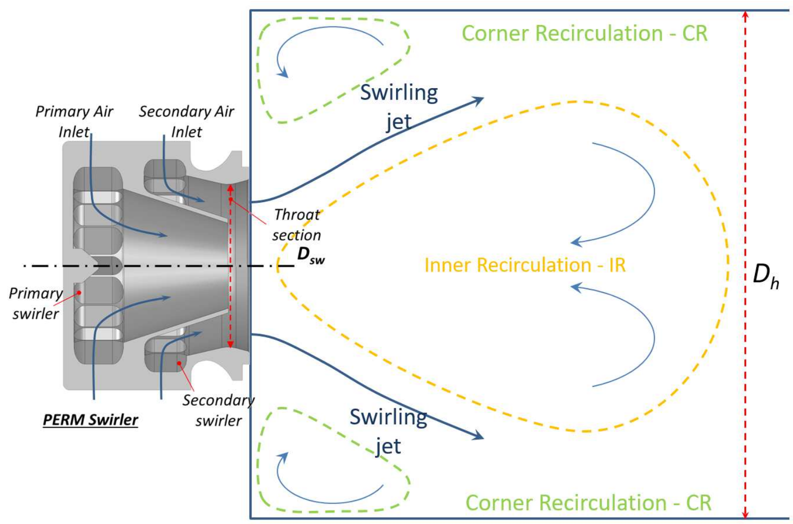

Figure 3: Geometry of the adopted swirler injectors

of a central toroidal recirculation region, can be established by a proper sizing of the swirling intensity of the flow. The common criteria is to introduce the so-called Swirl Number (S_N) which is defined as the ratio between the axial flux of circumferential momentum G_θ and the axial momentum flux G_x:

$$S_N = \frac{G_\theta}{R_0 G_x} \quad (1)$$

where R_0 represents a characteristic dimension of the swirler. A Swirl Number greater than 0.5-0.6 may result in strong not equilibrated radial and axial pressure gradients which induce main vortex collapse (breakdown).

As discussed in Marinov et al. [31], a swirl number of 0.75 is prescribed at the throat section of the investigated nozzles ($R_0 = 0.5D_{sw}$), with a highly uniform velocity distribution along the tangential direction. A fundamental geometric parameter affecting the stability of the flame by acting on the size of the central recirculation region, is the expansion ratio (see for instance Fu et al. [33] or Andrews et al. [34]) defined as the ratio between combustion chamber hydraulic diameter and nozzle diameter (D_h/D_{sw} according to Figure 3): a value of 2.5 can be observed in the case of PERM design. All the features of the PERM injector discussed above allow to generate a flow field that can be considered representative of a typical lean direct injection burning system for modern aero-engine combustors.

2.3. PSP technique

In order to estimate the film covering performance of the three effusion geometries and to evaluate the mutual effects between coolant and the mainstream swirled flow, a Pressure Sensitive Paint technique was employed in the central region of the liner.

Thanks to the luminescence behaviour due to their chemical composition, PSP can be exploited as a reliable detector of fluid oxygen concentration close to the paint layer and hence used for film effectiveness measurements based on heat and mass transfer analogy (gas concentration technique). Since the governing equations for heat and mass transfer phenomena are similar, the solutions of the two analogous problems are identical if the boundary conditions are the same and if the molecular/turbulent Schmidt number are identical to molecular/turbulent Prandtl number (i.e. Lewis number equal to one). As reported by several authors, turbulent flow are characterized by a turbulent Lewis number roughly equal to one as required by the analogy [35]. Regarding the applicability of the heat and mass transfer analogy in the investigated case - effusion cooling with highly swirled turbulent flow and cooling jets in penetration regime - the mixing process is mainly located far from the test plate where the turbulence effects are dominant, and hence the analogy can be considered satisfied. It is worth notice that, even if the hypothesis of unity turbulent Lewis is usually met, the similarity of molecular diffusion may not be satisfied. In the present test case the molecular quantities influence the heat and mass transfer phenomena in the viscous sub layer near the wall. However, a lower influence of molecular parameter in this region is expected due to the zero concentration/temperature gradient at the adiabatic/non-permeable liner wall.

Therefore, assuming valid the heat and mass transfer analogy and using a tracer gas without free oxygen as coolant, is possible to estimate the adiabatic film cooling effectiveness distribution on the liner [36] according to the following equations:

$$\eta_{ad} = \frac{T_{main} - T_{aw}}{T_{main} - T_{cool}} \equiv \frac{C_{main} - C_w}{C_{main}} \tag{2}$$

where C_{main} and C_w are oxygen concentration respectively in the main free stream and in proximity of the wall.

For further information, an extensive description of the technique operating principles and the experimental procedure are reported in previous works conducted by the authors [37][28].

As shown in Figure 4, the central region of the liner geometry was sprayed with several light coats of

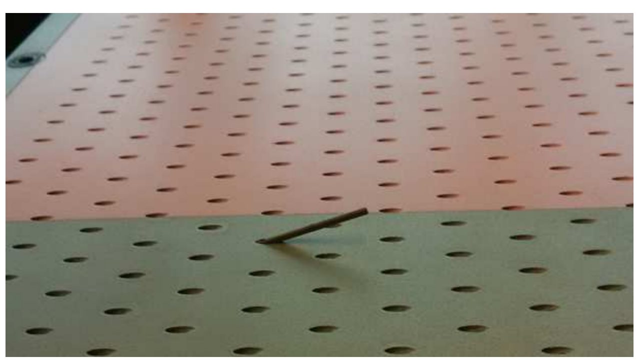

Figure 4: 20° effusion plate covered with PSP

PSP. The paint employed was provided by Innovative Scientific Solutions Inc., and it was composed by a blend of Fluoro Isopropyl Butyl polymer (FIB) and Platinum tetra(pentafluorophenyl) porphyrin (PtTFPP). During realized tests the paint was excited with an high performance led illuminator DLR-IL104®and the emission was captured by a 1600x1200 resolution 14-bit CCD camera PCO.1600. The selected foreign gas used to perform adiabatic film cooling effectiveness tests is nitrogen. Two dedicated feeding lines, equipped with calibrated orifices, are employed to feed the effusion and the slot plenum chamber, from a 10bar pressure tank where the N_2 is stored.

The uncertainty of adiabatic film cooling effectiveness measurements was evaluated following the method proposed by Kline and McClintock [38], achieving values around 10% for $\eta_{ad} = 0.2$ and 3% for regions where $\eta_{ad} > 0.8$.

2.4. PIV measurements

Particle Image Velocimetry campaign was aimed at supporting the adiabatic film cooling effectiveness measurements in order to deeply understand the complex interactions between main swirled flow and the cooling flows. For this purpose three investigation planes were selected: the first, *Center* plane, is the meridian projection perpendicular to the liner test plate and passing trough the center of the central swirler, while the second, *Median* plane, is parallel to combustor liner passing through the axis of the injector and finally the third is the *Wall* plane located 5mm above the liner (Figure 5). With the effusion cooling flow enabled, PIV measurements were realized on center plane only, focusing the attention on the corner region underneath the central injector. The laser sheet (1mm thickness) was introduced through the top side PMMA window involving the use of a 45° inclined mirror, while the optical access for the camera was obtained from one of the transparent lateral walls. As a tracer, 1μm diameter olive oil particles were used, employing a Laskin nozzle for their generation. The injection takes place, through a perforated pipe, immediately downstream of the rig inlet bell mouth, alongside its whole height.

Two different camera/laser positions were necessary to cover, with enough image resolution, the estab-

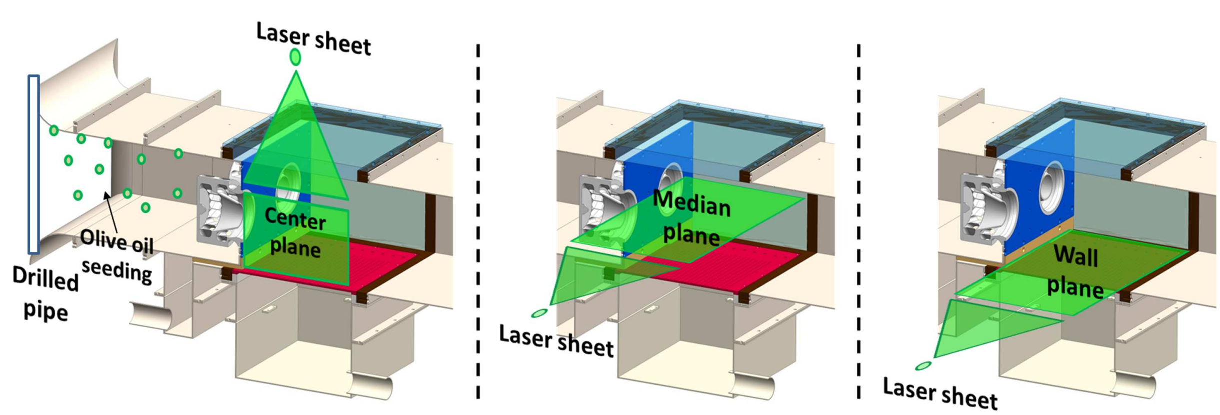

Figure 5: Position of the PIV measurement planes

lished investigation area, including a $5mm$ overlap to avoid loss of information in the neighbouring regions. A large number of image pairs were acquired, setting a time delay between the two laser pulses of about $10\mu s$, finally an iterative procedure based on an adaptive cross-correlation method was performed to obtain the velocity field distributions. Measurements were carried out using a Dantec Dynamics PIV system, based on a $120mJ$ New Wave Solo Nd:YAG pulsed laser (wavelength of $532nm$). For the effusion geometry with 30° holes inclination angle, a FlowSense $2Mpixel$ camera operating at a data rate of $15Hz$ was employed, with control and post-processing operations managed by means of the commercial software Dantec FlowManager®. For the other two multi-perforated plates was involved a SpeedSense $4Mpixel$ camera, coupled with the Dantec Dynamic Studio®. software.

Employing the method proposed by Westerweel [39] and considering a particle displacements varying from 5 to 10 pixels, measurements uncertainty in the mean velocity is estimated around 3%.

2.5. Test conditions

PSP measurements were conducted for all the three effusion geometries characterized by different injection angle, while PIV investigation wasn't performed for the 20° configuration because not significant variations were expected with respect to the already tested 30°. The whole experimental campaign was performed imposing representative operating flow conditions both for the mainstream and the cooling lines and replicating the relevant non dimensional parameters. The pressure drop across the set of swirlers was evaluated by means of multiple static pressure taps located upstream the dome (P_{in}) and downstream the investigated liner region near the outlet section (P_{out}). The pressure drop was maintained constant at the reference value of 3.5%:

$$\frac{\Delta P}{P} = \frac{P_{in} - P_{out}}{P_{in}} \tag{3}$$

With the imposed pressure drop, values of mainstream Reynolds number of about 160000 were achieved, considering the hydraulic diameter of the test section ($D_h/d = 260$) as the reference length. Regarding the cooling line, first focussing on the effusion system, the coolant was set acting on the pressure drop across the plate:

$$\Delta P/P_{eff} = \frac{P_{eff} - P_{out}}{P_{eff}} \tag{4}$$

where P_{eff} represent the static pressure measured inside the feeding plenum. Different different mass flow rates were tested, with the reference effusion pressure drop set at 3%. The pressure drop across the perforation was selected as the controlling parameter of coolant flow according to the operations of the real engine. Regarding the slot system, the test conditions are imposed through the coolant consumption parameter W, defined as the ratio between slot and mainstream mass flow rate related to the central swirler.

$$W = \frac{\dot{m}_{slot}}{\dot{m}_{main}} \cdot \frac{3}{2} \tag{5}$$

Tests were carried out for two levels of coolant consumption: with slot system disabled and with the actual combustor flow split $W = 3\%$. Highest Reynolds number of effusion jets, obtained with the maximum

Main flow	Effusion flow	Slot flow
Air	$N_2 - Air(PIV)$	$N_2 - Air(PIV)$
$T_{main} = 300K$	$T_{eff} = 300K$	$T_{slot} = 300K$
$Re_{main} = 160000$	$Re_{eff} = 0 - 4000$	$Re_{slot} = 0 - 3500$
$\Delta P/P = 3.5\%$	$\Delta P/P_{eff} = 0 - 1 - 2 - 3\%$	$W = 0 - 3\%$

Table 1: Test matrix

pressure drop, is 4000, while for the slot mass flow the greatest Reynolds, based on slot height, is 3500.

For the whole experimental campaign, mainstream flow is air at ambient conditions, regarding the coolant flows, air is employed for PIV test while Nitrogen was used to perform PSP measurements resulting in a coolant to mainstream density ratio equal to 1.

During the commissioning phase of the test rig, the three test plates where separately flow checked imposing the same conditions in terms of tested pressure drop in order to asses the values of discharge coefficients (Cd). The two test plates with slant injection angle highlighted a Cd approximately equal to 0.67, while the normal hole perforation exhibited an higher discharge coefficient close to 0.75 as already documented by Others in the open literature [40].

Each geometry was tested at the same pressure drop levels. According to the different effective areas of the perforations, the 20° and 30° plates have a ratio between effusion and mainstream mass flow on the central sector in the range $7.5-13\%$ when varying the $\Delta P/P_{eff}$, on the other hand the coolant consumption for the plate with normal holes is in the range $8.4-14.5\%$. All the test conditions are summarized in Table 1.

The main issue related to the adopted test conditions is the reduced level of density ratio with respect to expected actual engine condition ($DR \approx 2.5$). The density ratio has an impact on the adiabatic film cooling effectiveness distribution particularly in the transition between mass addiction and penetration regime and its effect seems to be negligible in full penetration regime [41]. These aspects have been already debated by the Authors by means of a dedicated experimental survey using effusion plates with uniform flow conditions [22]. However, considering the expected effusion flow field, mainly in penetration regime, and the pure comparative purpose of the survey, the main outcomes of the work can be considered unaffected by the lack of DR similitude.

3. Results

3.1. Flow field investigation - Case without effusion cooling

Before analyzing the behaviour of the effusion cooling process, a description of the flow field generated by the adopted swirlers will be reported. According to its high swirl number and expansion factor, the swirling jet delivered by the nozzles quickly breakdown when entering in the chamber, with the generation of a large inner recirculation region. As a consequence of the abrupt change in cross section, the swirling jets trigger two recirculating regions in the outer corners between liners and heat shield. An high speed annular swirling jet is observed between central and corner recirculations. Such flow structures are clearly shown in Figure 6 where flow field measured by the described PIV technique is reported on the previously defined Center plane: the value U_{max} used to normalize the velocity is, for all the shown maps, 50 m/s. The near wall region up to effusion row 14 is interested by a very complex flow field which is expected to heavily affect the development of the film. In particular it can be observed a reverse flow up to the $5th$ row, due to corner recirculation, followed by a stagnation area where the swirling jet collides with the liner (between rows 5 and 8). Downstream of the $8th$ row a strong flow acceleration can be observed, while after row 14 the flow begins to develop in a smoother way. As it will clearly results from the discussion of adiabatic film effectiveness measurements, a significant impact on effusion cooling jets mixing is observed in this region.

To better understand the swirler flow field, the results obtained on an additional PIV frame are shown in Figure 7 which shows the streamlines on the median plane. Thanks to this visualization the complete

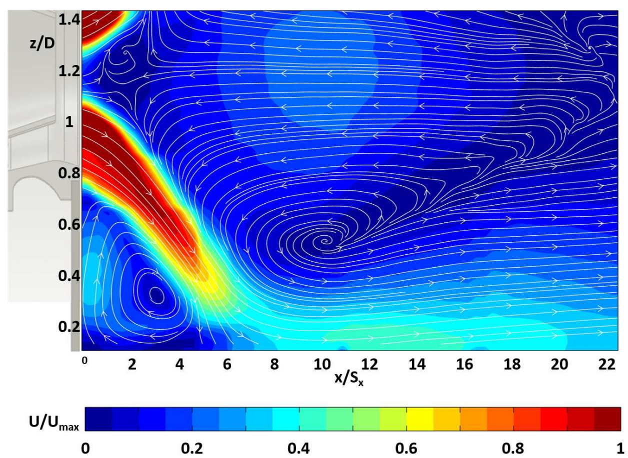

Figure 6: Flow field with no coolant injection on the central meridian plane

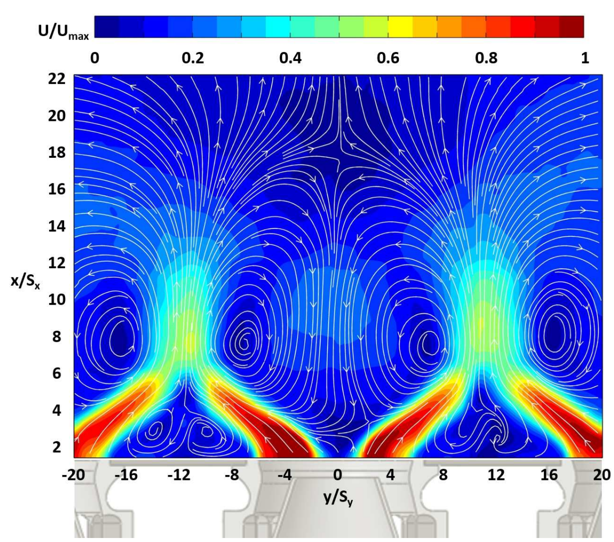

Figure 7: Flow field with no coolant injection on the median plane

extension of the central recirculation regions can be clearly pointed out. It is also important to observe the almost exact symmetry of the inner recirculation generated by the central nozzle respect to swirler axis. This finding confirms the proper design of the rig with representative results coming from investigations on the central sector.

Contour plot depicted in Figure 8 highlights the main flow direction close to liner surface: reverse flow is observed upstream of the stagnation region, while more downstream the flow is gradually loosing the residual swirling component. This velocity map will be used in the following to provide an estimation of effusion jets Blowing Ratio.

Exploiting available CFD results obtained on the present geometry with an Hybrid RANS/LES approach, which proved to perfectly match the measured flow field (see Mazzei et al. [42] for additional details), more quantitative evaluations of the flow field were carried out. First of all the swirl number in the throat section of the central nozzle was verified. According to the definition provided in previous sections, the computed swirl number is 0.77 which is fairly close to the nominal expected design value of 0.75. Mass flow rates entering into the inner region, $\dot{m}_{IR}$, and into the corner region, $\dot{m}_{CR}$, are computed to be respectively 57% and 38% of the mass flow delivered by the swirler.

3.2. Flow field investigation - Effect of effusion cooling

Results of Figure 9 highlight deep modifications in the flow field varying the coolant injection angle and strong interaction phenomena near the wall between the mainstream and the cooling flows. A different extension of the investigation area was achieved for the two configurations, both covering however the region

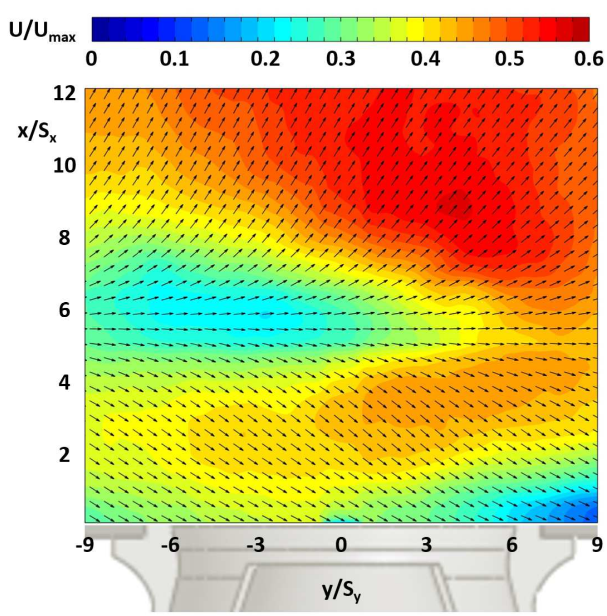

Figure 8: Flow field with no coolant injection on wall plane. Length of vectors are not proportional to velocity magnitude

of greater interest near the heat shield and liner corner. As expected minor discrepancies are observed in the the main recirculation region.

As already shown in [28], two well-distinct counter rotating vortices are generated by the 30° geometry with only the effusion system activated, while enabling the slot injection a coherent flow structure with high and positive velocity components in the axial direction is established. In this condition, the slot system seems to have a positive effect on film covering development inhibiting reverse flow near the liner.

Observing the corner regions in the 90° configuration with effusion coolant injection, a clockwise vortex can still be recognized as in the no cooling case. Nevertheless the high momentum of effusion jets in the positive z direction pushes the vortex center more downstream and closer to liner. A disturbing effect of this strong flow interaction is expected in terms of film cooling effectiveness in the early part of the liner. For $W = 3\%$ condition, slot coolant doesn't exhibits enough axial momentum to prevail on orthogonal effusion jets and is early lifted up, generating a low velocity region established near the heat shield underneath the swirling jet. However, similarly to 30° plate, slot injection tends to destroy the clockwise corner vortex, accomplishing only positive velocity components in the x direction near the wall.

As a general result, the 90° perforation tends to lift up the swirler jet, reducing its opening angle and

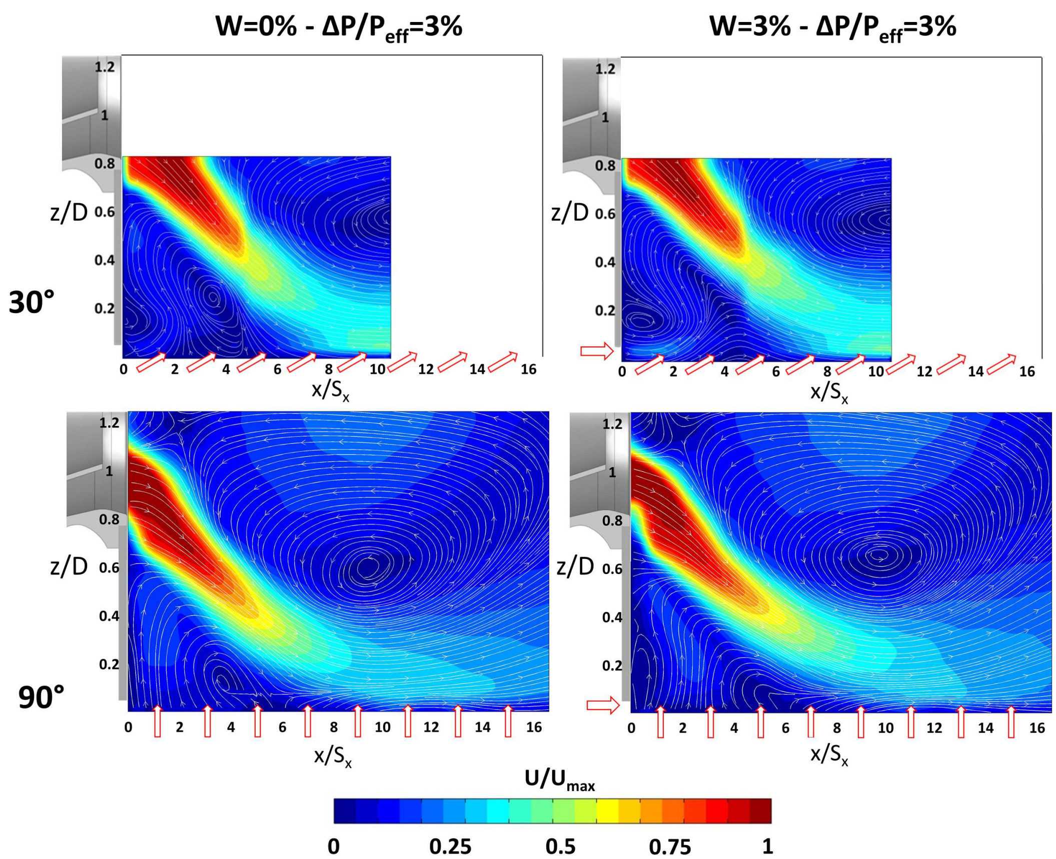

Figure 9: PIV results: flow field on measurements plane

moving slightly downstream the impingement region on the liner.

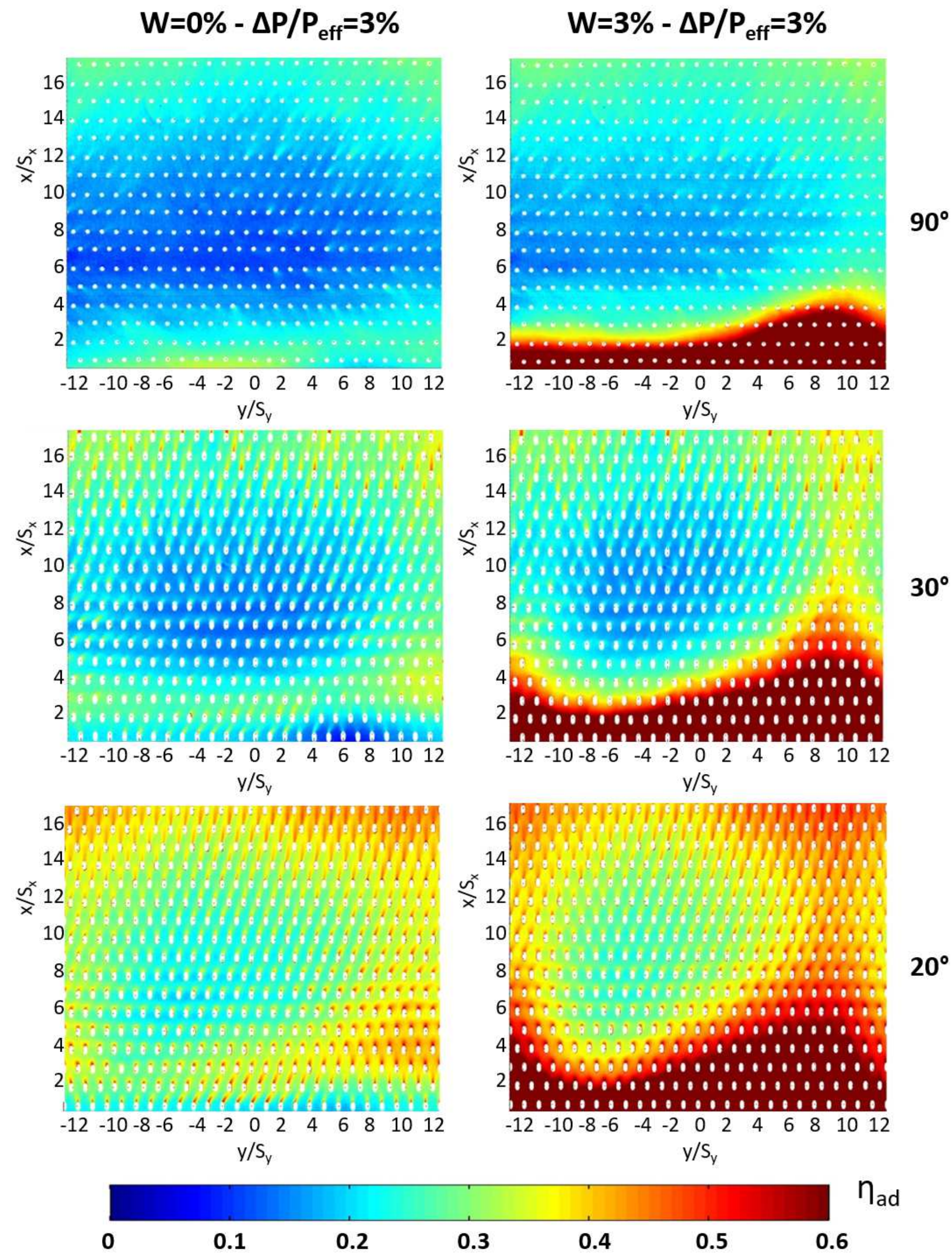

Figure 10: Adiabatic film cooling effectiveness distributions

3.3. Adiabatic film cooling effectiveness measurements

PSP campaign was aimed at investigating the adiabatic film cooling effectiveness distributions of three effusion plates under representative swirling flow, in order to explore the effect of injection angle on film covering. Tests were conducted imposing the swirlers pressure drop at the reference condition of $\Delta P/P = 3.5\%$. Effusion mass flow rates were set on the basis of multi-perforated plates pressure drop: three conditions were investigated corresponding to $\Delta P/P_{eff} = 1\%, 2\%, 3\%$. For each geometry, one test with slot cooling enabled was carried out in concurrence of the maximum level of effusion injection.

In Figure 10 are respectively reported from left to right the 2-D maps of η_{ad} obtained for 20°, 30° and 90° injection angle with a reference value of $\Delta P/P_{eff}$ equal to 3%. Distributions on the left column were obtained with the slot system disabled, while for the right column ones a coolant consumption equal to $W = 3\%$ was set. All maps are characterized by a non-symmetric central region with low effectiveness, corresponding to the stagnation region of the impinging jet highlighted by the PIV measurements. It is also worth to notice that probably part of the coolant is entrapped in the dome recirculation structures and is responsible of generating a streak with high effectiveness between about $y/S_y = 7$ and $y/S_y = 11$.

As expected, the highest film covering is achieved by the geometry with the lower inclination angle,

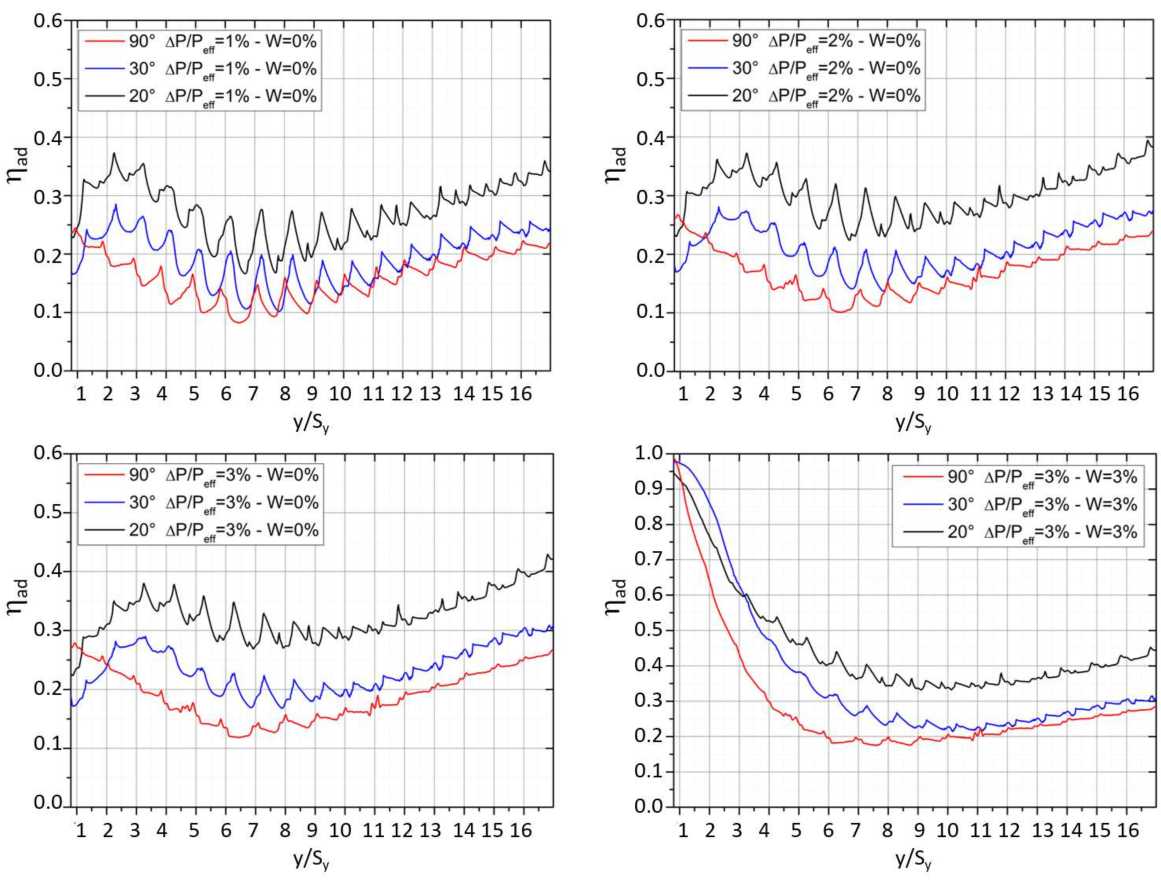

Figure 11: Laterally averaged adiabatic film cooling effectiveness profiles

where the coolant slant injection is capable to limit jet penetration and to take benefit from superposition effects. The high resolution color maps obtained allow to appreciate the different shape of coolant wall traces produced by each jet. Longer and more defined coolant imprints are observed for 20° geometry, while for 90° coolant traces appears less coherent and more sensible to mainstream flow field.

The importance of using the slot system to start the film protection is clearly stated in the right column distributions with an high film protection region obtained for $x/S_x < 2$. The role of slot cooling is appreciable up to the jet stagnation region, while downstream approaching the exit, its effect is almost negligible.

For a more quantitative analysis, the laterally averaged distributions of adiabatic film cooling effectiveness are reported in Figure 11. A comparison between the three multi-perforated plates is shown for all the three levels of effusion mass flow rate, with the slot disabled, and for the reference condition with both the cooling systems activated.

Apart from the expected increase of the film effectiveness in the final part of the liner ($x/S_x > 14$) when cooling flow rate is increased (alongside with $\Delta P/P_{eff}$), similar evolution is observed for all the tested conditions. Minimum adiabatic film cooling effectiveness values are clearly detected in the swirling jet stagnation region ($x/S_x \approx 7$) due to the high turbulence levels generated by impingement phenomena that tends to destroy the film and to lift up the effusion flow. Downstream ($x/S_x > 9 - 10$), superposition effect leads to an almost linear growth of η_{ad} allowing to guarantee sufficient film protection also for the lower effusion mass flow rates.

Results confirm the superiority of the 20° geometry in almost all the liner, with the gap versus the other configurations that tends to increase enhancing the $\Delta P/P_{eff}$. With respect to 30° angle, a mean gain of about 30% is achieved in terms of averaged film effectiveness with the 20° geometry. In the very first part of the liner ($x/S_x < 2$) good results are also obtained by the 90° configuration due to the presence of reverse flow near the wall, that leads to upstream film covering produced by the first rows of holes.

Distributions concerning the tests with slot coolant injected report approximately unitary values at the liner entrance with the 30° plates showing the best results up to $x/S_x = 3$. Differences between the film protection generated by the 30° and 90° inclination angle are appreciable in the first part of the liner ($x/S_x < 9$), while downstream the values are almost comparable. The behaviour of the 90° test case with slot injection in the early part of the liner is a consequence of the observed premature film lift up due to strong flow recirculation (see 9): adiabatic film effectiveness values for normal holes plate are roughly half of the values registered for the 20° case at rows 3-4.

A more comprehensive understanding of the obtained results can be achieved by the observation of the Blowing Ratio distribution along the effusion cooling rows. A direct measure of the velocity at the outlet of each effusion cooling hole was not possible and therefore BR is obtained assuming an uniform mass flow rate across the perforation. This assumption is justified by the presence of a feeding plenum upstream of the effusion plate and to small pressure variations on the mainstream side. The variation of BR along the plate is therefore related mainly to the distribution of mainstream velocity close to liner wall. According

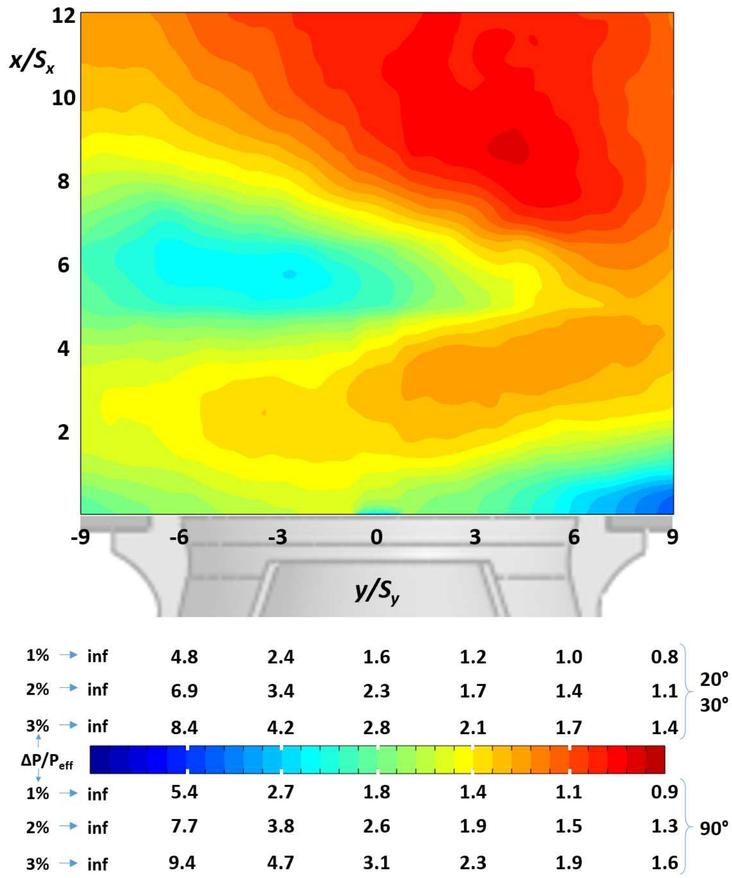

Figure 12: Distribution of the reference Blowing Ratio throughout the liner for the different cases investigated

to the mainstream velocity map obtained by PIV measurement on the Wall plane obtained with no coolant injection (Figure 8), it is possible to draw a distribution of a reference BR throughout the plate. Wall plane was considered as the reference location for mainstream velocity because it is located just at the outer edge of the slot (whose height is $5mm$): this plane also represents the nearest location to liner surface where the effect of effusion cooling jets is no longer observed. Reference BR is computed as follows:

$$BR = \frac{\frac{\dot{m}_{eff}}{A_{eff}}}{\rho V_{main}} \tag{6}$$

where $\dot{m}_{eff}$ is the effusion cooling mass flow, A_{eff} is the geometric cross section of the effusion perforation while ρV_{main} is obtained assuming a constant density in the mainstream and taking the velocity from the PIV wall plane measurements. Figure 12 shows the distribution of the above defined BR, with different scales for each level of pressure drop across the effusion plates (which implies different $\dot{m}_{eff}$) distinguishing between 90° and 20°-30° according to the different discharge coefficients. It can be observed that, at the nominal level of effusion pressure drop (3%), the reference BR is always above 1.5 for all the cases, with values between 4-5 observed in the low mainstream velocity region of swirling jet impingement. The assumption of full penetration state for the film cooling regime is therefore definitely confirmed.

Focusing the attention on the initial part of the liner, the three maps of Figure 13 allow to deepen the impact of the slot system varying the effusion angle. The top figure shows the adiabatic film cooling effectiveness distribution obtained with only the slot system activated with the holes of the effusion plates plugged on the rear side to avoid air ingestion. Map is relative to the 90° geometry but an analogous behaviour was comprehensibly achieved also for the other configurations. A significant non-symmetric distribution in tangential direction is observed due to the macro flow structure which affects the test section and tends to direct towards the right side the flow near the liner surface [27], resulting in an high film protection region up to the third row of holes between $y/S_y \approx 5$ and $y/S_y \approx 10$. In the remaining parts of the map, high adiabatic film cooling effectiveness values are limited to the first row of holes.

The two following maps of Figure 13 were respectively obtained with 90° and 20° geometries and were carried out with both the slot and effusion system set at their reference conditions. Nevertheless, in this case the multi-perforated plates were fed with air, instead of Nitrogen, in order to take into account the fluid dynamic effect of coolant injection through the liner perforation without contributing to film protection detection (no free-oxygen tracer). Both the two distributions highlight a significant positive effect produced by effusion flow on the contribution of the slot coolant to the global film protection. In particular, the slant

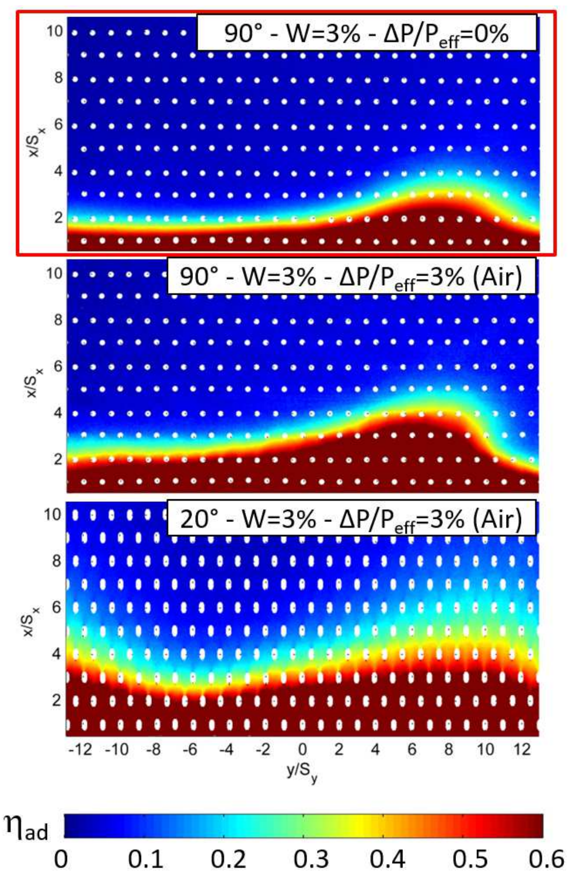

Figure 13: Adiabatic effectiveness distributions: slot injection

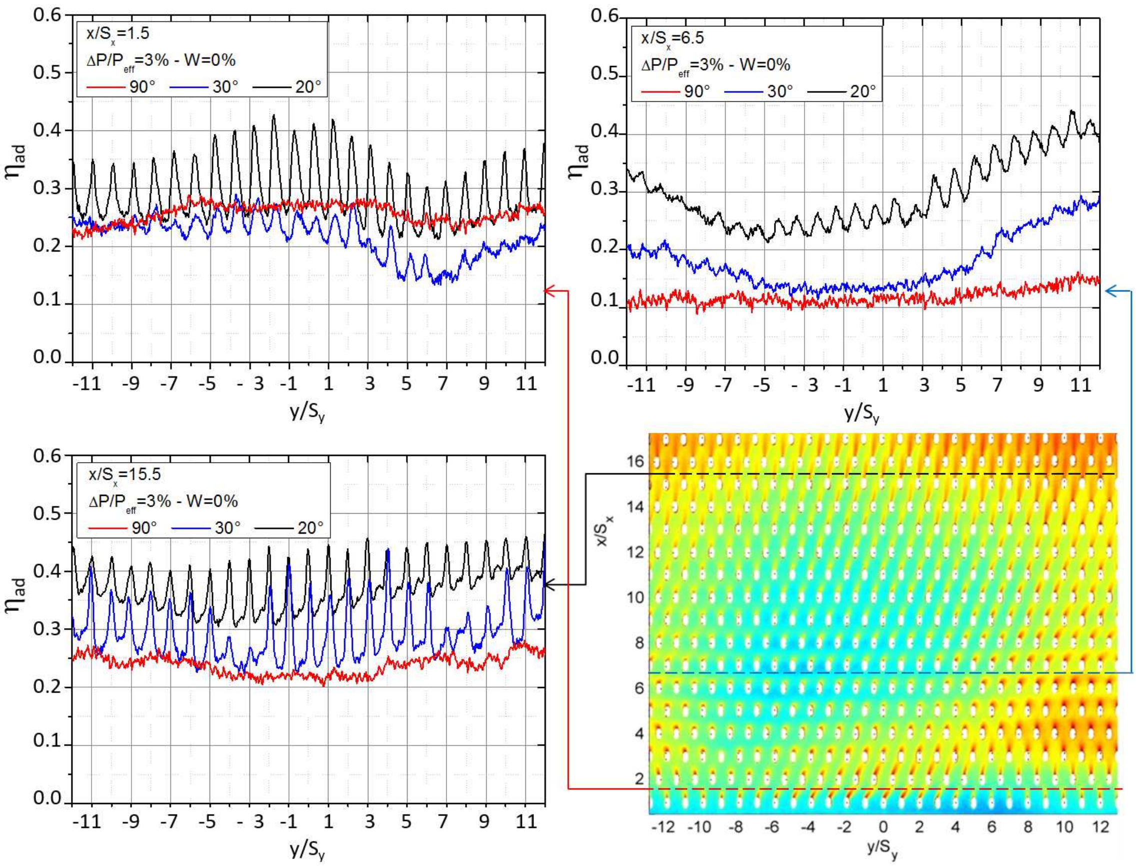

Figure 14: Lateral profiles of adiabatic effectiveness extracted at different axial positions

injection of the 20° liner produces inclined jets with high momentum that tend to energize the coolant flow structure exiting from the slot and to drag downstream its effect. Moreover, the distribution seems to be less affected by the test section flow field with a more constant behaviour alongside the y direction and with a film protection destroyed more gradually respect to the plate with perpendicular holes.

To better understand the behaviour of effusion film, three lateral profiles of adiabatic effectiveness have been extracted and reported in Figure 14: plots highlight the effect of the coolant injection angle at the more representative axial positions $x/S_x = 1.5; 6.5; 15.5$, respectively in the corner region, in the impingement zone and in the last part of the plate with more uniform flow structures. In the corner vortex region, the 90° plate shows film effectiveness values higher respect to the 30° especially in the $3 < y/S_y < 9$ zone where the slant angle performance seems strongly affected by the dome vortex structures. The superiority of the 20° plate is clearly represented in the impingement region where, despite the strong interactions with the main flow, the jets still present well defined coolant traces downstream of the injection points, especially for $y/S_y > 0$. It is interesting to observe that the 90° plate is not able to produce the high effectiveness streak at $y/S_y > 6$ and the η_{ad} is almost constant around the value 0.1. Finally, at $x/S_x = 15.5$ where the main flow field is more uniform the slant injection plates show their potentiality with pronounced and extended film traces.

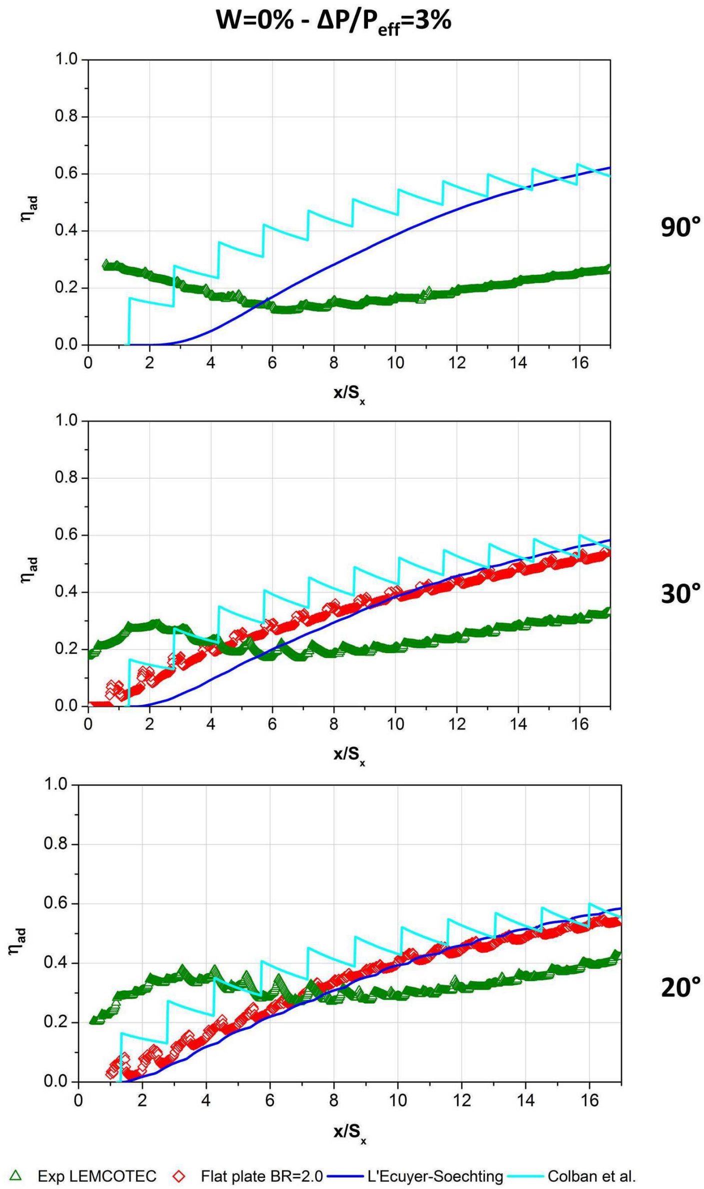

Figure 15: Comparisons of adiabatic film effectiveness measured in the present experimental campaign with literature correlations and experimental results obtained with a uniform mainstream velocity (only 20° and 30° cases)

3.4. Comparison with literature correlations

In order to assess how common literature correlations for adiabatic film effectiveness could be a reliable tool for the prediction of the investigated configurations, a comparison with formulas proposed by L'Ecuyer and Soechting [41] and by Colban et al. [43] was carried out. Both correlations are valid for a single row of holes on flat plate: the evaluation of the film effectiveness over the entire multi-perforated liner is realized by assuming a superposition of the contributions predicted for each row, recalling the superposition criteria proposed by Sellers [44]. The correlation proposed by L'Ecuyer and Soechting is based on a large database of experimental results for standard cylindrical holes with inclination angles between 30° and 90°. The correlation proposed by Colban and coworkers was developed to predict adiabatic film effectiveness with common fan shaped holes, but it can be used also for not shaped cylindrical perforations: in this case no explicit dependency on the inclination angle is accounted in the expression.

Correlations were applied by assuming a uniform distribution of the measured mass flow rate over the perforations, while the velocity evolution along the axial direction on the mainstream side was obtained by laterally averaging the module of velocity retrieved by PIV measurements on the Wall plane (see 5): the resulting blowing ratios for the effusion cooling rows in each case are exactly equivalent to values reported in 12. Results for the three investigated cases at $\Delta P/P_{eff} = 3\%$ without slot cooling injection are shown in 15.

As additional term of comparison, for inclined holes only (20° and 30°), 15 shows the measured adiabatic film effectiveness obtained on the same hardware and with the same measurement technique but removing the swirlers and therefore prescribing a uniform velocity in the mainstream. In these cases a constant blowing ratio is obtained and the considered value (2.0) represents an averaged of the values observed for inclined cases in the three sector rig. It is interesting to point out the quite good agreement between correlations and experiments with uniform mainstream, confirming the reliability of the used correlations and of the assumption of full superposition in presence of simple mainstream flow. On the contrary, when a realistic swirling flow is considered, correlations are not able to properly catch the adiabatic film evolution in the early part of liner affected by mainstream flow recirculation (upstream rows 6-7). Downstream the stagnation region of the swirling jet, when the combustor mainstream starts to assume a more uniform behaviour, the adiabatic film begins to point out a row by row superposition with a rate similar to what predicted by correlations and to what observed in the simple flat plate configurations, as confirmed by an equivalent slope of adiabatic film effectiveness curves along the x direction. This observation suggests a possible fruitful use of simple correlations at least in the final part of the multiperforated liner.

4. Conclusions

An experimental study was presented dealing with the impact of holes injection angle on the performance of an effusion cooling system. Test were conducted under realistic flow field conditions in a non-reactive three sector planar rig equipped with a lean burn swirler injectors and a complete cooling scheme composed of a slot for starter film cooling and a multi-perforated liner. The work was focused on the adiabatic film cooling effectiveness measurement for three effusion plates with different injection angle (20°, 30°, 90°) under several cooling conditions. A PSP technique was exploited to obtain detailed η_{ad} distributions and a supplementary PIV survey was carried out to support the analysis.

Velocity maps show an apparently critical behaviour for the 90° injection angle where the orthogonal coolant injection seems to be subjected to an high penetration in the mainstream, generating streamlines oriented mainly in the z direction and leading to a premature lifting of the slot coolant. On the other hand a slant injection from the effusion system helps the development of a more coherent slot coolant stream and avoids the generation of reverse flow near the liner wall.

Adiabatic film cooling effectiveness maps show a deep impact of the injection angle on the effusion system performance. As expected, the more tilted geometry (20°) leads to the best film protection, revealing a better opposition to the coolant layer destruction caused by the impinging swirl jet and showing an advantageous exploitation of superposition effects thanks to the limited penetration of the cooling jets. Furthermore the slanted injection of effusion coolant has a beneficial impact on the slot system, extending more downstream its effects.

In conclusion, the experimental survey allowed to deeply characterize a typical effusion system and to investigated the impact of coolant injection angle on adiabatic film cooling effectiveness distribution. The interaction with a typical combustion chamber flow field and the coexistence with other cooling method, as the slot starter film cooling, were also analysed, providing fundamental information for the design of modern combustor cooling scheme.

Acknoledgement

The authors wish to gratefully acknowledge LEMCOTEC (Low Emissions Core-Engine Technologies) Consortium for the kind permission of publishing the results herein. LEMCOTEC is a Collaborative Project co-funded by the European Commission within the Seventh Framework Programme (2007-2013) under the Grant Agreement n 283216.

References

[1] S. M. Correa, Power generation and aeropropulsion gas turbines: From combustion science to combustion technology, Symposium (International) on Combustion 27 (2) (1998) 1793–1807.

[2] H.-J. Bauer, New low emission strategies and combustor designs for civil aeroengine applications, Progress in Computational Fluid Dynamics, An International Journal 4 (3-5) (2004) 130–142.

[3] R. Krewinkel, A review of gas turbine effusion cooling studies, International Journal of Heat and Mass Transfer 66 (2013) 706 – 722.

[4] M. Martiny, A. Schulz, S. Wittig, Mathematical model describing the coupled heat transfer in effusion cooled combustor walls, ASME Conference Proceedings (97-GT-329).

[5] M. Gerendás, K. Hoeschler, S. Th., Development and Modeling of Angled Effusion Cooling for the BR715 Low Emission Staged Combustor Core Demonstrator, RTO AVT Symposium on "Advanced Flow Management: Part B - Heat Transfer and Cooling in Propulsion and Power Systems" .

[6] A. Andreini, R. Becchi, B. Facchini, L. Mazzei, A. Picchi, A. Peschiulli, Effusion cooling system optimization for modern lean burn combustor, ASME Conference Proceedings (GT2016-57721).

[7] N. Kasagi, M. Hirata, M. Kumada, Studies of full-coverage film cooling - 1. cooling effectiveness of thermally conductive wall, American Society of Mechanical Engineers (Paper) (81 -GT-37).

[8] G. E. Andrews, A. A. Asere, M. L. Gupta, M. C. Mkpadi, Effusion cooling: the influence of number of hole, Journal of Power and Energy **204**.

[9] G. E. Andrews, A. A. Asere, M. L. Gupta, M. C. Mkpadi, A. Tirmahi, Full Coverage Discrete Hole Film Cooling: The Influence of the Number of Holes and Pressure Loss, ASME Conference Proceedings (90-GT-61).

[10] G. E. Andrews, I. M. Khalifa, A. A. Asere, F. Bazdidi-Tehrani, Full Coverage Effusion Film Cooling With Inclined Holes, ASME Conference Proceedings (95-GT-274).

[11] M. Martiny, A. Schulz, S. Wittig, Full-coverage film cooling investigations: adiabatic wall temperatures and flow visualization, ASME Conference Proceedings (95-WA/HT-4).

[12] K. M. B. Gustafsson, T. Johansson, An Experimental Study of Surface Temperature Distribution on Effusion-Cooled Plates, J. Eng. Gas Turbines Power. **123** (2001) 308–316.

[13] M. K. Harrington, M. A. McWaters, D. G. Bogard, C. A. Lemmon, K. A. Thole, Full-Coverage Film Cooling With Short Normal Injection Holes, J. Turbomach. 123 (2001) 798–805.

[14] A. Martin, S. J. Thorpe, Experiments on Combustor Effusion Cooling Under Conditions of Very High Free-Stream Turbulence, ASME Conference Proceedings (GT2012-68863).

[15] J. J. Scrittore, K. A. Thole, S. Burd, Investigation of Velocity Profiles for Effusion Cooling of a Combustor Liner, ASME Conference Proceedings (GT2006-90532).

[16] P. Ligrani, M. Goodro, M. Fox, H.-K. Moon, Full-Coverage Film Cooling: Film Effectiveness and Heat Transfer Coefficients for Dense and Sparse Hole Arrays at Different Blowing Ratios, J. Turbomach. 134 (6) (2012) 061039.

[17] N. W. Foster, D. Lampard, The Flow and Film Cooling Effectiveness Following Injection through a Row of Holes, Journal of Engineering for Power 102 (3) (1980) 584.

[18] C. A. Hale, M. W. Plesniak, S. Ramadhyani, Film Cooling Effectiveness for Short Film Cooling Holes Fed by a Narrow Plenum, J. Turbomach. 122 (3) (2000) 553.

[19] S. Baldauf, A. Schulz, S. Wittig, High-Resolution Measurements of Local Effectiveness From Discrete Hole Film Cooling, J. Turbomach. 123 (4) (2001) 758.

[20] C. Yuen, R. Martinez-Botas, Film cooling characteristics of rows of round holes at various streamwise angles in a crossflow: Part I. Effectiveness, International Journal of Heat and Mass Transfer 48 (23-24) (2005) 4995–5016.

[21] T. Behrendt, C. Hassa, M. Gerendás, Characterization of Advanced Combustor Cooling Concept Under Realistic Operating Conditions, ASME Conference Proceedings (GT2008-51191).

[22] A. Andreini, B. Facchini, A. Picchi, L. Tarchi, F. Turrini, Experimental and theoretical investigation of thermal effectiveness in multiperforated plates for combustor liner effusion cooling, J. Turbomach. 136 (9).

[23] J. J. Scrittore, K. A. Thole, S. Burd, Experimental Characterization of Film-Cooling Effectiveness NearCombustor Dilution Holes, ASME Conference Proceedings (GT2005-68704).

[24] A. Ceccherini, B. Facchini, L. Tarchi, L. Toni, D. Coutandin, Combined Effect of Slot Injection, Effusion Array and Dilution Hole on the Cooling Performance of a Real Combustor Liner, ASME Conference Proceedings (GT2009-48845).

[25] B. Wurm, A. Schulz, H. J. Bauer, M. Gerendás, Impact of Swirl Flow on the Cooling Performance of an Effusion Cooled Combustor Liner, J. Eng. Gas Turbines Power. 134 (12) (2012) 121503–121503.

[26] B. Wurm, A. Schulz, H. J. Bauer, M. Gerendás, Cooling Efficiency for Assessing the Cooling Performance of an Effusion Cooled Combustor Liner, ASME Conference Proceedings (GT2013-94304).

[27] A. Andreini, G. Caciolli, B. Facchini, A. Picchi, F. Turrini, Experimental Investigation of the Flow Field and the Heat Transfer on a Scaled Cooled Combustor Liner With Realistic Swirling Flow Generated by a Lean-Burn Injection System, J. Turbomach. 137 (3) (2014) 031012–031012, ISSN 0889-504X.

[28] A. Andreini, R. Becchi, B. Facchini, L. Mazzei, A. Picchi, F. Turrini, Adiabatic Effectiveness and Flow Field Measurements in a Realistic Effusion Cooled Lean Burn Combustor, J. Eng. Gas Turbines Power. 138 (3) (2015) 031506–031506, ISSN 0742-4795.

[29] B. Ge, Y. Ji, Z. Chi, S. Zang, Effusion cooling characteristics of a model combustor liner at non-reacting/reacting flow conditions, Applied Thermal Engineering 113 (2017) 902 – 911, ISSN 1359-4311.

[30] LEMCOTEC Low Emissions Core-Engine Technologies, `http://http://www.lemcotec.eu/`, 2011-2016.

[31] S. Marinov, M. Kern, K. Merkle, N. Zarzalis, A. Peschiulli, F. Turrini, On Swirl Stabilized Flame Characteristics Near The Weak Extinction Limit, ASME Conference Proceedings (GT2010-22335).

[32] D. Lilley, Swirl Flows in Combustion: a Review, AIAA J. 15 (8).

[33] Y. Fu, J. Cai, S.-M. Jeng, H. Mongia, Confinement effects on the swirling flow of a counter-rotating swirl cup, ASME Conference Proceedings (GT2005-68622).

[34] G. E. Andrews, N. Ahmed, R. Phylaktou, P. King, Weak extinction in low NOx gas turbine combustion, ASME Conference Proceedings (2009) GT2009–59830.

[35] R. L. Simpson, R. L. Field, A Note on the Turbulent Schmidt and Lewis Numbers in a Boundary Layer, International Journal of Heat and Mass Transfer 15 (1972) 177–180,.

[36] T. V. Jones, Theory for the use of foreign gas in simulating film cooling, International Journal of Heat and Fluid Flow 20 (1999) 349–354.

[37] G. Caciolli, B. Facchini, A. Picchi, L. Tarchi, Comparison between PSP and TLC steady state techniques for adiabatic effectiveness measurement on a multiperforated plate, Experimental Thermal and Fluid Science 48 (0) (2013) 122–133.

[38] S. J. Kline, F. A. McClintock, Describing Uncertainties in Single Sample Experiments, Mechanical Engineering 75 (1953) 3–8.

[39] J. Westerweel, Fundamentals of digital particle image velocimetry, Measurement Science and Technology 8 (12) (1997) 1379–1392.

[40] M. Gritsch, A. Schulz, S. Wittig, Effect of Crossflows on the Discharge Coefficient of Film Cooling Holes With Varying Angles of Inclination and Orientation, J. Turbomach. 123 (4) (2001) 781–787.

[41] M. R. L'Ecuyer, F. O. Soechting, A model for correlating flat plate film cooling effectiveness forrows of round holes, in: AGARD Heat Transfer and Cooling in Gas Turbines 12p (SEE N86-29823 21-07), 1985.

[42] L. Mazzei, A. Andreini, B. Facchini, F. Turrini, Impact of Swirl Flow on Combustor Liner Heat Transfer and Cooling: A Numerical Investigation With Hybrid Reynolds-Averaged Navier–Stokes Large Eddy Simulation Models, J. Eng. Gas Turbines Power. 138 (5) (2016) 051504.

[43] W. F. Colban, K. A. Thole, D. Bogard, A film-cooling correlation for shaped holes on a flat-plate surface, Journal of Turbomachinery 133 (1) (2011) 011002.

[44] J. P. Sellers, Gaseous Film Cooling with Multiple Injection Stations, AIAA Journal 1 (9) (1963) 2154–2156.